On the Effect of Local Barrier Height in Scanning Tunneling Microscopy: Measurement Methods and Control Implications

UT Dallas Author(s):

Farid Tajaddodianfar
S. O. Reza Moheimani

Citation:

Tajaddodianfar, F., S. O. Reza Moheimani, J. Owen, and J. N. Randall. 2018. "On the effect of local barrier height in scanning tunneling microscopy: Measurement methods and control implications." Review of Scientific Instruments 89(1), doi:10.1063/1.5003851

On the effect of local barrier height in scanning tunneling microscopy: Measurement methods and control implications

Farid Tajaddodianfar, S. O. Reza Moheimani, James Owen, and John N. Randall

Citation: Review of Scientific Instruments **89**, 013701 (2018); doi: 10.1063/1.5003851
View online: https://doi.org/10.1063/1.5003851
View Table of Contents: http://aip.scitation.org/toc/rsi/89/1
Published by the American Institute of Physics

On the effect of local barrier height in scanning tunneling microscopy: Measurement methods and control implications

Farid Tajaddodianfar,[1,a)] S. O. Reza Moheimani,[1,b)] James Owen,[2,c)] and John N. Randall[2,d)]
[1]*Department of Mechanical Engineering, Erik Jonsson School of Engineering and Computer Science, The University of Texas at Dallas, Richardson, Texas 75080, USA*
[2]*Zyvex Labs LLC, 1301 N Plano Rd., Richardson, Texas 75081, USA*

(Received 8 September 2017; accepted 11 December 2017; published online 2 January 2018)

A common cause of tip-sample crashes in a Scanning Tunneling Microscope (STM) operating in constant current mode is the poor performance of its feedback control system. We show that there is a direct link between the Local Barrier Height (LBH) and robustness of the feedback control loop. A method known as the "gap modulation method" was proposed in the early STM studies for estimating the LBH. We show that the obtained measurements are affected by controller parameters and propose an alternative method which we prove to produce LBH measurements independent of the controller dynamics. We use the obtained LBH estimation to continuously update the gains of a STM proportional-integral (PI) controller and show that while tuning the PI gains, the closed-loop system tolerates larger variations of LBH without experiencing instability. We report experimental results, conducted on two STM scanners, to establish the efficiency of the proposed PI tuning approach. Improved feedback stability is believed to help in avoiding the tip/sample crash in STMs. *Published by AIP Publishing.* https://doi.org/10.1063/1.5003851

I. INTRODUCTION

The invention of the Scanning Tunneling Microscope (STM) in the early 1980s facilitated the study of material surface physics by providing atomic-resolution surface images.[1] Since its invention, the STM has found many applications in surface and material science which have led to a number of ground breaking observations.[2–5] In addition to being a diagnostic tool, the STM is now being used for lithography which makes it a strong candidate as a tool for atomically precise manufacturing in the future.[6,7]

The functionality of the STM is based on a quantum mechanical phenomenon known as the tunneling current which refers to the electrical current established between an atomically sharp tip and a conducting surface when their relative distance is in the order of 1 nm and a direct current (DC) bias voltage is established between the two objects. The tunneling current is exponentially dependent on the tip/sample separation under a constant bias.[1] Therefore, a linear control system can be implemented to measure the logarithm of the current and move the tip in a direction normal to the sample to regulate the current at a constant setpoint.[1,8] This is the basis for operation of the STM in constant current mode which provides a topographic image of the surface.

Under normal imaging conditions, the relative distance between the tip and the sample is in the range of a few angstroms.[9] At such extreme proximity and due to the presence of adverse effects such as the highly resonant nature of piezo-actuators, model uncertainties and nonlinear dynamics, precise operation of the control system is of vital importance. Otherwise, a tip/sample crash may occur which dulls the tip and damages the sample. Although attempts to use advanced controllers, e.g., sliding mode control,[10] have been reported, proportional-integral (PI) control is the primary feedback control system used in STMs.[8,11,12] The PI controller with fixed gains may occasionally lose its safe performance due to large uncertainties in STM dynamics. Hence, poor performance of the control system can be a major cause of tip/sample crashes which is a well-known operational challenge in STMs.

Following early applications in imaging, the STM tip was found to be useful as a tool for triggering chemical reactions selectively at distinct locations on the sample. Specifically, the STM is used in Hydrogen Depassivation Lithography (HDL) during which the STM tip transmits a tunneling current which is large enough to remove surface hydrogen by breaking its bond to silicon.[13–16] Commonly, both current setpoint and bias voltage are higher in the lithography mode compared to the imaging mode.[6,7] The tip-sample crash problem due to the poor control performance can be even worse in the lithography mode given the larger uncertainties caused by ongoing chemical reactions on the surface.

This work is aimed at addressing the tip/sample crash issue in STMs by improving the control system performance both in imaging and lithography modes. Previously, we presented a method for closed-loop system identification which enabled us to obtain the open-loop dynamics of the STM.[17] We showed that the DC gain of the open-loop system is strongly affected by the Local Barrier Height (LBH), which depends on the quantum mechanical properties of the tip and local surface atoms, and hence is not constant.[18] LBH and its variable nature have been known to the STM users and have been studied extensively for several decades.[9,19,20] Additionally,

a)Electronic mail: farid.tajaddodianfar@utdallas.edu
b)Author to whom correspondence should be addressed: reza.moheimani@utdallas.edu
c)Electronic mail: jowen@zyvexlabs.com
d)Electronic mail: jrandall@zyvexlabs.com

a procedure known as the "gap modulation method" has been used to estimate the LBH and simultaneously to construct an image to plot the LBH variations over the sample surface.[1,20]

The gap modulation method or dI/dZ spectroscopy refers to the procedure during which the tip-sample separation is oscillated at a known frequency and the resulting oscillation in the logarithm of current is tracked by a lock-in amplifier. In this approach, it is assumed that the modulating frequency is beyond the controller bandwidth, and hence the tip/sample oscillating amplitude is assumed to be constant.[1,9] However, this is a weak assumption that does not always hold. Consequently, the LBH obtained through this approach can be affected by feedback parameters. Furthermore, this assumption is contradictory to the requirement of high-bandwidth controllers for fast scanning purposes.[21]

In this paper, we modify the gap modulation method based on the insight that the DC gain of the open-loop system is a strong function of the LBH. In the method proposed here, we use two lock-in amplifiers to track the dither signal at the input and output ports of the system simultaneously in order to obtain a more accurate estimation of the LBH. In addition, we present experimental results comparing the conventional and proposed LBH estimation methods. They show that our proposed method results in LBH images with less dependence on the feedback parameters. We observe that surface features with higher LBH are more easily distinguished from the topographic features using our proposed method.

LBH is assumed to be constant in the design of STM control systems.[8,10,11,22,23] However, this assumption is inconsistent with the variable nature of the LBH and may lead to closed-loop instabilities in STMs.[18,24] We propose to continuously update the PI controller gains in order to preserve the closed-loop stability despite variations in the LBH. We present experimental results that show how a feedback system with fixed controller gains can experience instability over specific locations on the sample where the true value of the LBH is different from those for which the controller gains were selected. We report experimental results that show over the same locations our auto-tuning PI controller preserves closed-loop stability and leads to a superior performance. All the experiments are performed on hydrogen passivated silicon surfaces.

In the remainder of the paper, we present theoretical insights into the STM control system operation and the conventional gap modulation method in Sec. II. Then, we state our approach to LBH measurements and propose a self-tuning PI control scheme based on the estimated LBH. In Sec. III, we present experimental results that show the efficiency of our LBH estimation method as well as the self-tuning controller. We conclude the paper in Sec. IV.

II. THEORETICAL INSIGHTS

In this section, we briefly describe the commonly used gap modulation method for LBH estimation that dates back to the early STM studies in the 1980s.[1] We will describe an alternative solution that we believe to lead to superior results. We discuss the implications of inaccurate LBH measurement on the stability of the STM control system and explain how our proposed method can lead to a high-performance control system.

A. Conventional LBH measurement method

It is well-known that assuming a constant small bias voltage V with a one-dimensional square barrier of height φ above the Fermi level results in a simplified tunneling current model[9]

$$i \propto V \exp\left(-1.025\delta\sqrt{\varphi}\right), \tag{1}$$

where δ in $\mathring{A}$ is the barrier thickness and is approximately equal to the tip-sample separation. The barrier height φ depends on the electronic properties of both the tip and the sample and usually is assumed as the average of the tip and sample work functions.[1] Theoretical and experimental investigations have shown that, in the typical working ranges of the STM, φ is almost independent of δ.[19] Therefore, in such ranges, a linear relationship holds between the logarithm of tunneling current ($\ln i$) and the tip-sample separation δ. This allows for the implementation of a linear feedback control system to keep the current i at a constant setpoint i_d by adjusting the relative distance between the tip and the sample.

The assumption that φ is independent of δ in the working range immediately converts Eq. (1) to the following relation that makes it possible to measure the barrier height:

$$\varphi \propto \left(\frac{d \ln i}{d\delta}\right)^2. \tag{2}$$

Equation (2) indicates that the rate of change of $\ln i$ with respect to the separation δ is proportional to the square root of the barrier height. The gap modulation method was introduced in the early STM studies to measure φ based on Eq. (2). In this method, a modulating signal at frequency Ω is added to the piezo-tube drive and forces the tip to oscillate in the direction normal to the sample. It is assumed that the oscillation amplitude of δ at that frequency is fixed because Ω is beyond the bandwidth of the controller. Then only tracking the amplitude of $\ln i$ at Ω using a lock-in amplifier will suffice to calculate φ.

The barrier height obtained by Eq. (2) is a quantity that depends on the surface local electronic properties as well as those of the tip. Hence, the terminology Local Barrier Height (LBH) or the apparent barrier height is used. This measurement is a basis to generate another STM image called the LBH image which is found to be capable of presenting additional details regarding the surface physics. However, the basic assumption that validates the gap-modulation method is not always correct. In fact, even if Ω is beyond the bandwidth of $K(s)$, there is always a portion of $\ln i$ at Ω which passes through the controller $K(s)$ and adds up to δ that is modulated at Ω. This means that $\ln i$ influences δ at frequency Ω and this effect becomes more profound when larger controller bandwidth is required for fast imaging. Under these circumstances, the denominator of Eq. (2) can no longer be assumed to be a constant and this may affect the measured LBH values.

In Sec. II B, we first discuss the effect of LBH on the controller stability and performance, and then we propose an alternative approach to LBH measurement to circumvent the above issues.

B. LBH effects on control system performance

Equation (2) shows that the LBH can be considered, mathematically, as a gain which maps the tip-sample gap (δ) into the logarithm of current ($\ln i$). Knowing that the current control system uses $\ln i$ as the feedback signal and adjusts δ by a control signal, it can be shown that the LBH is directly affecting the DC gain of the open-loop STM dynamics that is being controlled. There are other parameters that contribute to the plant DC gain, e.g., the high-voltage amplifier gain and piezo-material sensitivity. However, all of these parameters are fixed. In addition, it can be assumed that any dynamic drop due to the scanner and filter dynamics at the frequency of modulation is fixed. These assumptions are based on the closed-loop system identification tests performed on the STM which have been discussed in the authors' previous reports.[17,18,24]

Figure 1 displays a simplified block diagram of the STM Z-axis control. Here, $G(s)$ and $K(s)$ are the open-loop plant and controller dynamics, respectively. k_{HV} is the high-voltage amplifier gain and $G_p(s)$ is the piezo-scanner dynamics in the Z-direction. Surface topography, constant logarithm terms, and measurement noise are represented by h, C, and n, respectively, and i_d is the current setpoint.

It is well-known in that the DC gain of the open-loop plant is a critical factor in the closed-loop stability and performance of the system. Since the DC gain is a function of the LBH value, the STM stability can be violated if the LBH experiences substantial variations. In a previous work,[18] we presented experimental results which suggested that the DC gain may vary by a factor of two due to the LBH variations on a H-passivated silicon sample and a tungsten tip. Therefore, LBH variations can destabilize the STM feedback loop that operates based on a conventional fixed-gain PI controller.

C. Proposed LBH measurement method

Our approach for measuring the LBH is similar to the conventional method in the sense that it is based on modulating the tip-sample distance at a high frequency and tracking the corresponding amplitude at the output by a lock-in amplifier. However, unlike the conventional approach, we assume that the modulated amplitude of δ may change due to the controller response. This is a sensible assumption because even if the modulating frequency is out of the bandwidth of the closed-loop system, the controller will always pass a portion of $\ln i$ at the frequency Ω, and as a result, the modulation amplitude of δ will be affected by LBH.

The control block diagram shown in Fig. 1 motivates us to measure the DC gain of the plant $G(s)$ and relate it to the LBH variations. To do this, we inject a single-tone dither signal with frequency Ω at an arbitrary point in the feedback loop, e.g., current setpoint, and track the amplitude of Ω-components at the input and output of $G(s)$. If the amplitude of setpoint dither is r_0, the corresponding amplitudes at the input and output of $G(s)$ will be given by

$$Y(j\Omega) = K(j\Omega)G(j\Omega)\left(1 + K(j\Omega)G(j\Omega)\right)^{-1} r_0, \tag{3}$$

$$W(j\Omega) = K(j\Omega)\left(1 + K(j\Omega)G(j\Omega)\right)^{-1} r_0, \tag{4}$$

where $W(s)$ and $Y(s)$ are input and output signals for $G(s)$ in Laplace space, respectively, as shown in Fig. 2, and $j = \sqrt{-1}$. Calculating the magnitude of complex variables and dividing (3) by (4) gives

$$\frac{\| Y(j\Omega) \|}{\| W(j\Omega) \|} = \| G(j\Omega) \| = \widetilde{C}, \tag{5}$$

which means that the fraction in the left of (5) is independent of the controller dynamics and feedback effects and solely dependent on the plant dynamics at the frequency of Ω. On the other hand, we can separate the effect of the plant DC gain and the rest of its dynamics by re-writing the right hand as

$$\widetilde{C} = \sqrt{\varphi} k_{HV} \gamma \| G_0(j\Omega) \|, \tag{6}$$

where γ is the constant piezo-material sensitivity and $G_0(s)$ is a dynamic system with unit DC gain representing the remaining dynamic components of $G(s)$. As discussed before,[18] $\|G_0(j\Omega)\|$ is reasonably assumed to be constant during the

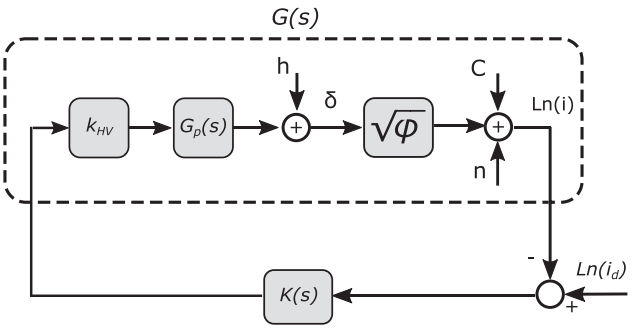

FIG. 1. Simplified Z-axis control block diagram showing the LBH as a parameter that affects the DC gain of open-loop plant $G(s)$.

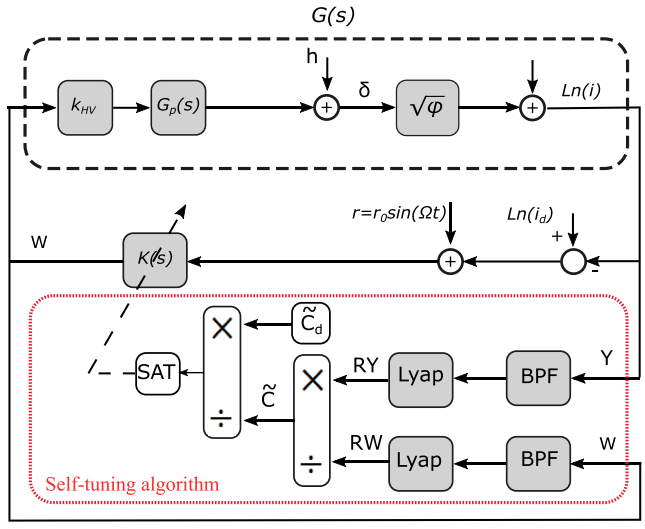

FIG. 2. The LBH is estimated by measuring the open-loop gain $\widetilde{C}$ at a fixed high frequency Ω. To do this, the current setpoint is modulated at the frequency Ω and the amplitude of the corresponding component at $\ln i$ and W are tracked by a lock-in amplifier and are divided by each other. A combination of a 2nd order IIR band-pass filter (BPF) and a 1st order Lyapunov filter is used to track the amplitudes at the modulation frequency Ω. By setting a user-defined constant value $\widetilde{C}_d$, a signal for continuous update of the PI controller gains is obtained as $\widetilde{C}_d/\widetilde{C}$ which is passed through a saturation box SAT for a safety reasons.

STM operation. Thus, any variation in $\widetilde{C}$ is due to the changes in the square root of LBH. We calculate $RY = \|Y(j\Omega)\|$ and $RW = \|W(j\Omega)\|$ using any type of lock-in amplifier and divide them to obtain $\widetilde{C}$ according to (5) at each time t. The estimated parameter $\widetilde{C}$ reflects the variations of the LBH and is proportional to the feedback loop gain. Therefore, $\widetilde{C}$ can also be used to continuously update the gains of a PI controller in reaction to variations in plant DC gain in order to maintain the LBH at a pre-determined level. Here, we use a Lyapunov filter to track the amplitude of the dither signal. This is an alternative implementation of a lock-in amplifier that was described in detail previously.[24,25] In this scheme, the signal is first passed through a second order infinite impulse response (IIR) band-path filter with a passband centered at Ω and then a first order Lyapunov filter tracks the amplitude of the resulting signal.

D. Self-tuning PI controller

Conventionally, a proportional-integral (PI) controller is used to regulate the current in STMs operating in constant current mode. Such a controller is described by two parameters: the integral gain k_i and the corner frequency ω_c,

$$K(s) = k_i \left(\frac{1}{s} + \frac{1}{\omega_c} \right). \tag{7}$$

With a fixed corner frequency, the feedback loop gain is a multiplication of k_i and the DC gain of $G(s)$. Hence, to minimize the effect of LBH variations on the feedback loop, we can update k_i continuously as follows:

$$(k_i)_{n+1} = (k_i)_n \frac{\widetilde{C}_d}{\left(\widetilde{C}\right)_n}, \tag{8}$$

which means that based on the value of $\widetilde{C}$ estimated at the step n, the integral gain at step $n+1$ should be updated according to 8. Note that the speed with which $\widetilde{C}$ can be estimated is bounded by the limited bandwidth of the estimator. This originates from limited passband of the BPFs and bandwidth of the Lyapunov filters. Wider bandwidth enables faster but noisier estimation, and a trade-off should be made on each system. The scanning speed should be selected so that PI gains can be updated in response to topographic LBH changes. For instance, a $\widetilde{C}$ estimator shown in 2 with a 400 Hz bandwidth takes 5 ms to settle in reaction to a step change in LBH. During this time, the tip has traveled less than 0.3 nm if the scanning speed is 60 nm/s. Higher scanning speed will require wider estimation bandwidths. For a discussion on various methods of high speed amplitude modulation, see Ref. 26.

III. EXPERIMENTAL RESULTS

In this section, we present our experimental results. First, we describe the experimental setup. Then, we present the results showing the difference between the conventional and proposed LBH measurement methods, and finally, we use the proposed LBH method for control system tuning and showcase its efficiency on the Zyvex Labs scanner as well as a commercial scanner.

A. Experimental setup

A series of experiments were performed using a novel STM scanner designed by Zyvex Labs. This is a three degree-of-freedom serial kinematic piezo-stack actuator shown in Fig. 3. This scanner provides a 4 mm motion range in the coarse positioning mode through a stick-slip mechanism with consistent steps as small as 1 nm that were measured with an interferometer. Also, during fine positioning, a range of 3×3 μm in the XY plane and 1.5 μm in the Z-direction is achieved with a resolution better than 2 pm. A second set of experiments were conducted using a ScientaOmicron VT STM.[27] This instrument uses a piezo-tube scanner for fine positioning in a range of $12 \times 12 \times 1.5$ μm with a resolution better than 1 pm. Coarse positioning of this scanner is obtained by a stick-slip mechanism that covers a range of 10 mm at each direction with individual steps no larger than 40 nm. In this product, a built-in eddy-current damping system is implemented for vibration isolation, which removes the need for an additional mechanical stage for vibration isolation.

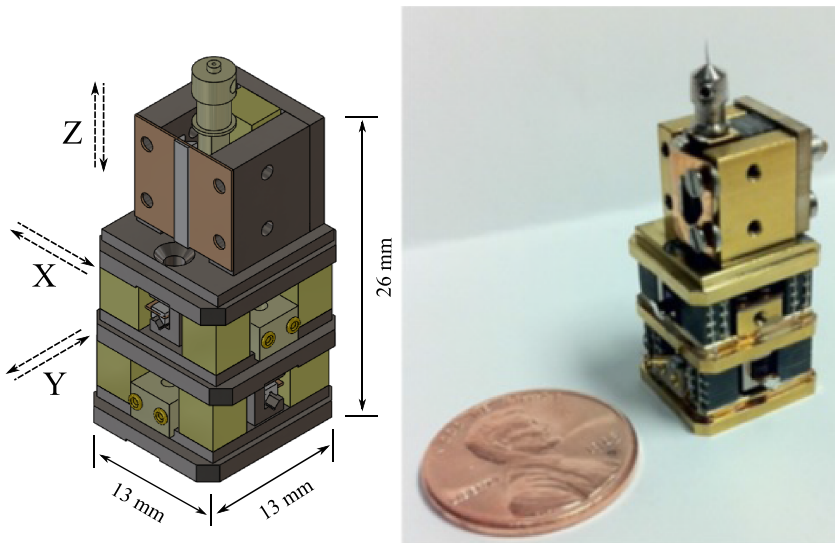

FIG. 3. Zyvex Labs' scanner: a serial kinematic piezo-stack actuator. Travel range is 4 mm × 4 mm × 4 mm (*XY Z*) and 3 μm × 3 μm × 1.5 μm (*XY Z*) for coarse and fine positioning, respectively.

Hydrogen terminated silicon samples with tungsten tips were used in the experiments. Details of sample preparation have already been presented in previous studies.[28] The STM is customized for Hydrogen Depassivation Lithography (HDL) which is previously described in detail.[6,28] Tip preparation is also discussed in a previous work.[29] All the experiments were conducted in the imaging mode; however, in several cases, lithography patterns are visible in the STM images.

Both of the scanners described above are operated in ultra-high vacuum of 10^{-11} Torr and in room temperature. A Femto DLPCA-200 current pre-amplifier with a gain of 10^9 Ω and bandwidth of 1 kHz is used for current measurement with the Zyvex scanner. A 20 bit Digital Signal Processing (DSP) unit running at 50 kHz sampling frequency is used for driving the system both in imaging and lithography modes. This DSP is a product of Zyvex Labs and is trademarked as ZyVector. A software unit called ScanZ provides the user with a graphical user interface as well as the capability to define scanning and lithography conditions, controller gains, and experiment conditions. The proposed LBH measurement and self-tuning control algorithms have been implemented in the DSP, and their parameters are tunable through ScanZ. A dSPACE MicroLabBox running at 50 kHz sampling rate is used for recording the time-domain data. The STM images presented in this paper are further processed by Gwyddion[30] for better display. Table I shows the main parameters used for imaging, LBH estimation, and controller tuning throughout this paper.

TABLE I. Major parameter values used throughout the experiments.

Parameter	Value
Feedback bandwidth	300 Hz
LBH estimation bandwidth	400 Hz
Rastering speed	60 nm/s
Dither frequency	4 kHz
Current setpoint	0.2 nA
Bias voltage	−2.5 V
Signal-to-noise ratio	10 dB

B. LBH measurement results

Both the conventional LBH measurement method and the alternative method proposed here are used to generate LBH images. These images are obtained with and without the PI controller tuning scheme described in Sec. II D. In the present section, we compare the obtained results to appreciate the difference between the two methods.

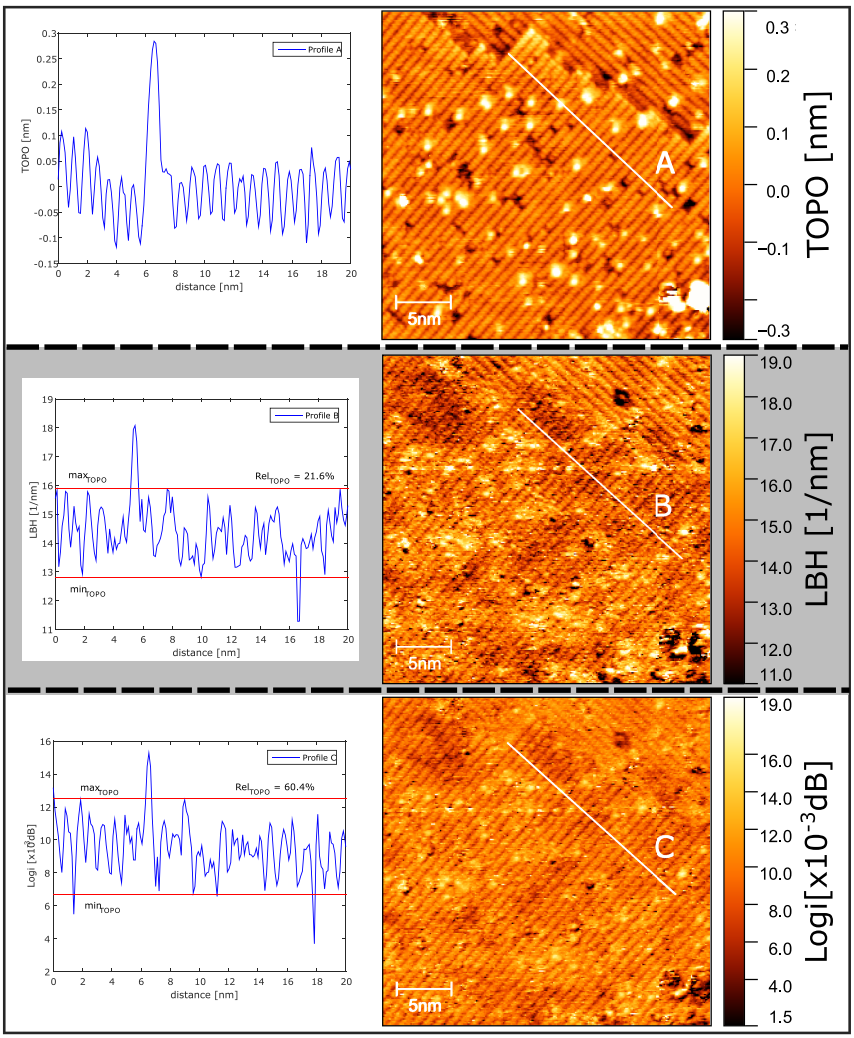

FIG. 4. STM topography image (top) and the LBH images using the proposed (middle) and the conventional (bottom) methods. All three images were captured simultaneously while the self-tuning algorithm was off. The plots left to each image show the corresponding profile and suggest that a relative 21.6% of the mean value is due to the topography effects in the proposed method, while this relative value is as high as 60.4% in the conventional method. A better contrast of LBH features in the conventional method is apparent. Rel_{TOPO} is defined as $Rel_{TOPO} = 2\,(max_{TOPO} - min_{TOPO})\,/(max_{TOPO} + min_{TOPO})$.

Figure 4 displays a STM topography image as well as LBH images obtained using the proposed and conventional methods simultaneously. Experiments were conducted with fixed PI gains. The topography image shows the relative height of features with respect to the mean value. In order to depict the LBH image, we estimated parameter $\widetilde{C}$ based on Eq. (6) and divided it further by the system constants k_{HV} and γ to set the units to 1/nm, as shown in Fig. 4 (middle). In the conventional method, only ln i is used to produce the image. The image displayed at the bottom of Fig. 4 was plotted using the signal RY shown in Fig. 2.

A number of surface features including dimer rows, a step edge, missing Si dimers, and dangling bonds (DB) are visible in the topography image (Fig. 4 top). For some features, the contrast is purely physical. The top of the step edge appears brighter than the base, while the missing dimer defects appear dark. Dangling bonds (DB) result from missing hydrogen atoms[6,28] and appear as bright features. In this case, the contrast is electronic. The dangling bond states are much closer to the Fermi level than the H-terminated dimers, and as a result, tunneling is easier on the dangling bonds; hence, the tunneling current tends to increase over them. However, since the controller keeps the current constant, it moves the tip away from the surface over a dangling bond and as a result dangling bonds appear as bright spots in the topography image. Equivalently, LBH is lower on a dangling bond since states are closer to the Fermi level. This results in a higher DC gain of $G(s)$ in Fig. 1 given the negative sign in the exponential component in Eq. (3).

It is well known that the LBH image is always correlated with the topography. One reason is that the control system moves the tip perpendicular to the average surface, while the actual current is not always in this direction.[1] Although the LBH changes while crossing the dimer rows, a large correlation to topography is considered an undesired effect in LBH images.[1] The profile B sketched in Fig. 4 (middle) shows that the topography is within 21.6% of the mean value of the recorded LBH, while the profile C shows this value as high as 60.4%, suggesting that the LBH image that our method produces presents less correlation to the topography. In addition, it is observed that the dangling bonds that are real LBH features appear with a better contrast in the middle image in Fig. 4 which suggests that the proposed method is capable of capturing the surface electronic properties with a better contrast.

Our analysis in Sec. II A shows that the conventional method also depends on the feedback system parameters, and we expect to observe more LBH image distortion while the

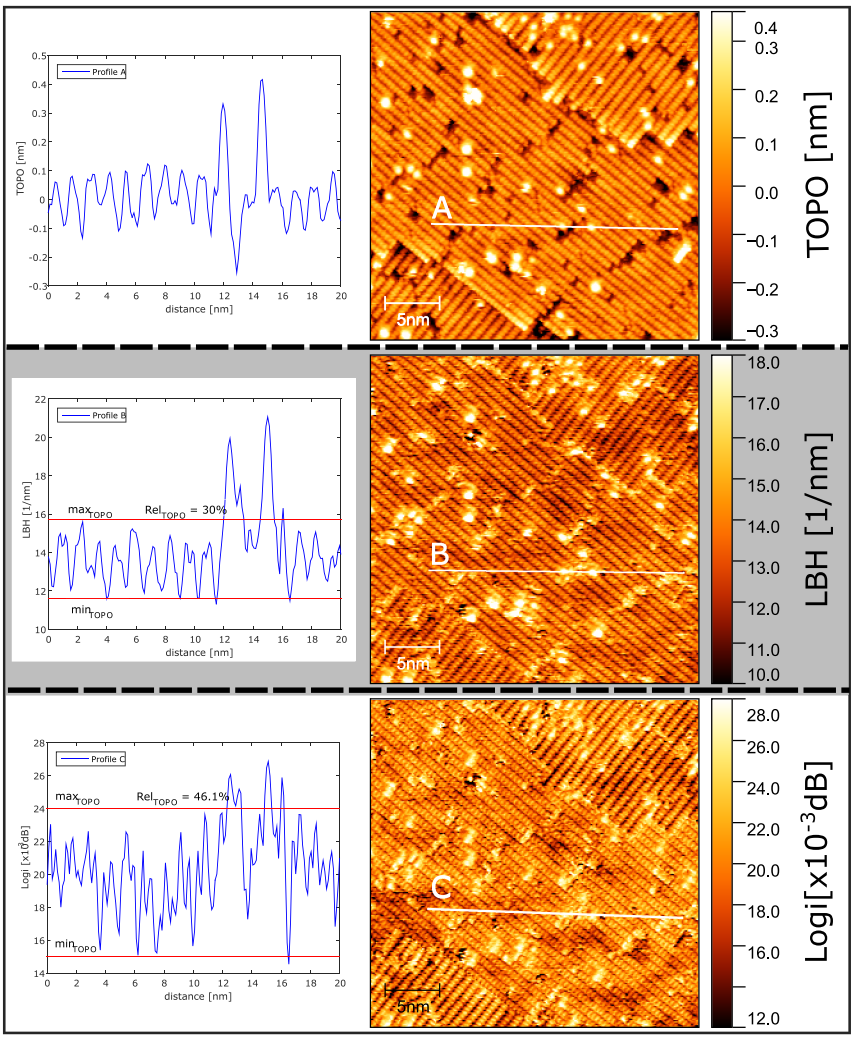

FIG. 5. STM topography image (top) and the LBH images using the proposed (middle) and the conventional (bottom) methods. All three images were captured simultaneously while the self-tuning algorithm was active. The plots left to each image show the corresponding profile and suggest that a relative 30.0% of the mean value is due to the topography effects in the proposed method, while this relative value is as high as 46.1% in the conventional method. It is clear that at the bottom image, the real LBH features appear as high as the topography features, but the LBH image obtained using our method (middle) is not affected by controller tuning and the LBH features are still distinguishable with good contrast.

controller gains are adjusted. This is shown in Fig. 5 which is the same as Fig. 4 except that the self-tuning control scheme proposed in Sec. II D is operating. Figure 5 (middle) shows that the LBH features are still distinguishable with good contrast while the self-tuning controller is operating. In contrast, in the ln (*i*) image which represents the conventional LBH measurement method, the LBH features appear as high as topographic features. This failure is due to the dependency of the conventional method on the feedback parameters, as discussed in Sec. II A.

C. Self-tuning PI control

In order to investigate the efficiency of the self-tuning algorithm proposed in Sec. II D, we assigned a set of high PI gains which put the feedback system close to the stability margin. We used the Zyvex Labs' scanner for these tests, and first turned the tuning algorithm off while scanning a litho-patterned sample with a slow rastering speed of 60 nm/s. In the patterned area, the LBH is higher than the rest of the sample. As a result, we expect the closed-loop system to experience ringing while passing over the litho-patterned area noting that the loop gain is already high.

Figure 6 displays the STM topography, current error, and LBH images on top, middle and bottom rows, respectively, for the two cases of PI tuning off (middle column) and on (right column). Prior to these tests, we produced a HDL pattern on the sample and drew several line patterns which are visible in the images plotted in Fig. 6. Hydrogen atoms have been removed from the patterned area. As a result, the LBH

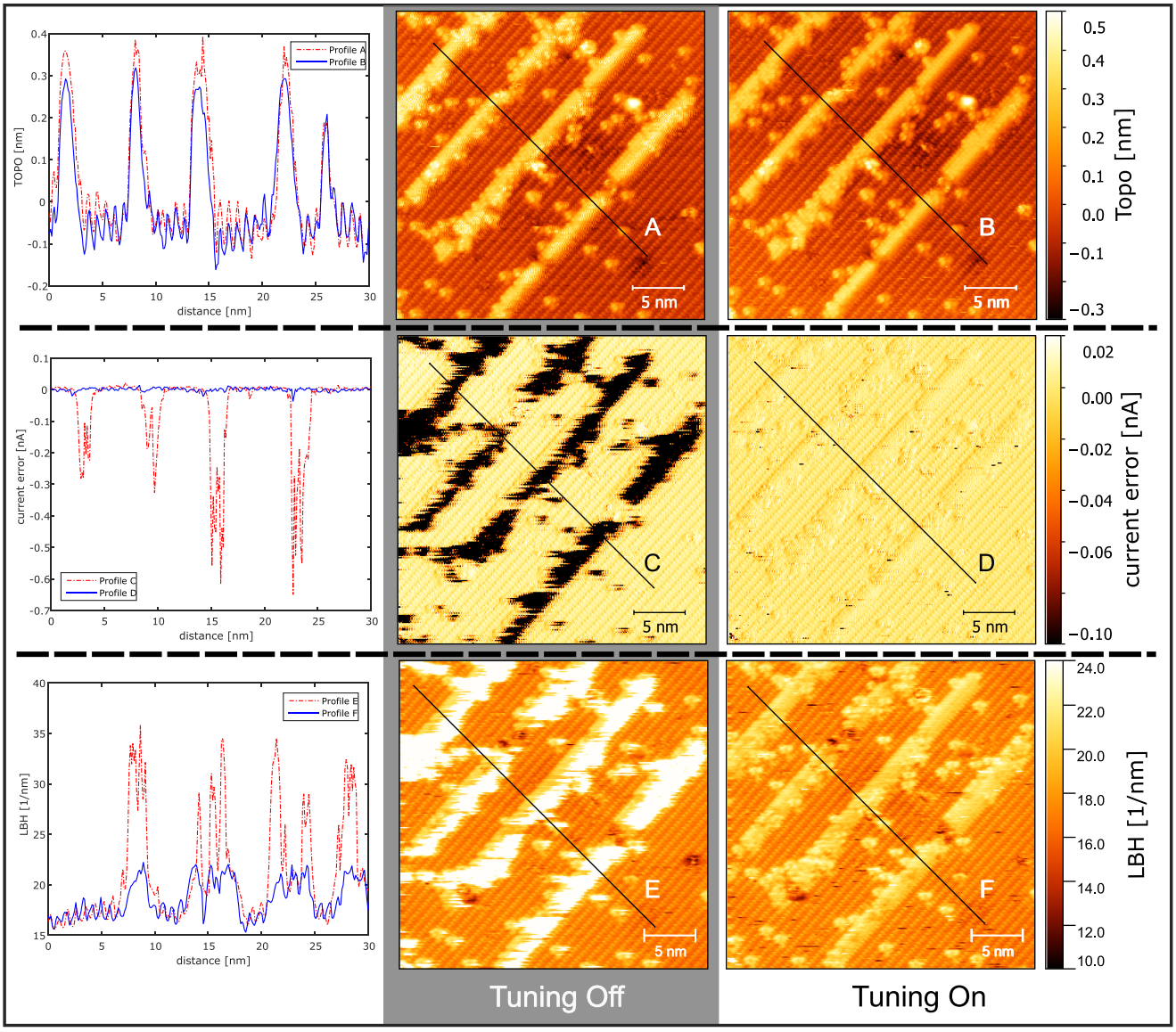

FIG. 6. Effect of the self-tuning PI controller using Zyvex Labs' scanner. Top: topography image, middle: current error image, and bottom: LBH image, for the two cases of tuning on (right column) and off (middle column). PI gains are high and the system is close to the stability margin when the tuning is off. Large feedback error proves closed-loop ringing and instability when passing over the lithography patterns. The same system with the self-tuning controller operating stays stable. Parameters given by Table I are used during the experiments. First, three images are captured simultaneously in one scan while the tuning was off. Immediately after that, we turned the tuning on and captured the images shown in the right column. All other parameters and scan conditions are the same between the two cases.

is higher on the patterns compared to the rest of the sample where electrons tunnel through hydrogen. Recalling that the LBH is directly affecting the closed-loop gain, we expect to observe instability over the patterns given large initial PI gains. We first fixed the PI gains and scanned the sample using the parameters given in Table I. Then, we activated the tuning algorithm and scanned the same area again. All other parameters and conditions are the same between the two successive scans.

The middle row of Fig. 6 compares the current error signal between the two cases. When the tuning is off, the feedback system undergoes large oscillations while passing over the lithography patterns. As a result, the current error experiences values as large as 0.6 nA. Note that in the areas other than the patterns, the system is stable and the current error is kept near zero. This supports our claim that the control system performance can be affected significantly by the local properties of the sample and tip. On the other hand, when the tuning is on, the current error image in the right column of Fig. 6 shows that the feedback stability is preserved both over the lithography patterns and hydrogen passivated area using the self-tuning algorithm.

The top row of Fig. 6 compares the topography images for the two cases with and without a self-tuning controller. Ringing due to the closed-loop instability is apparent around the patterns when the tuning is off. At the bottom row of Fig. 6, the LBH images are compared. Note that when the feedback system undergoes instability while the tuning is off, the LBH estimation algorithm fails. Therefore, the estimated LBH values shown in profile E are not reliable in this case. However, the system stays stable when using the PI tuning method. The estimated LBH values for this case displayed in profile F in Fig. 6 show a near 30% increase in the measured value which was enough to destabilize the feedback system in the absence of the tuning algorithm.

We also conducted further tests to verify the performance of the proposed self-tuning controller on the commercial Omicron scanner. We pursued the same test strategy articulated above by setting high PI gains and repeating the STM scan successively with and without the PI tuning scheme. Results are shown in Fig. 7. A prior lithography pattern provides an area on which the LBH value is locally different from the rest. Passing over the pattern while the tuning algorithm is off, the feedback system undergoes ringing as shown by profile D in Fig. 7 given that the PI gains are already high. However, repeating the same scan immediately with the self-tuning algorithm in operation, the control system preserves the stability as proved by the current error image and profile C in Fig. 7. Getting the same behavior on a commercial STM scanner assures us that the observed performance of the self-tuning PI controller is not due to the dynamics of the scanner and can be generalized to the whole family of STMs.

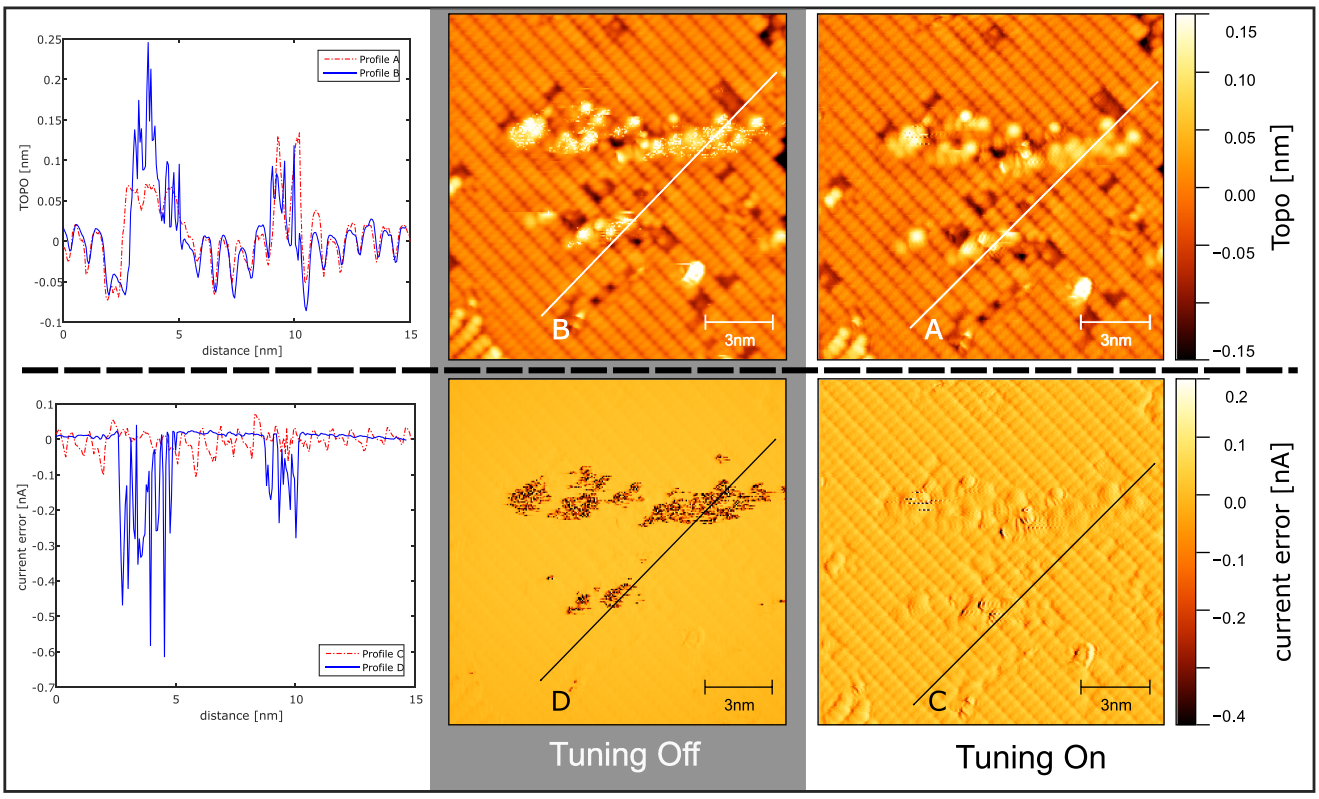

FIG. 7. Effect of the self-tuning PI controller using the Omicron scanner. Top: topography image, and bottom: current error image, for the two cases of tuning on (right column) and off (middle column). PI gains are high and the system is close to the stability margin when the tuning is off. Large feedback error proves closed-loop ringing and instability when passing over the lithography patterns. The same system with the self-tuning controller operating stays stable. Parameters given by Table I are used during the experiments. First, the two images in the middle column are captured simultaneously while the tuning was off. Immediately after that, we turned the tuning on and captured the images shown in the right column. All other parameters and scan conditions are the same between the two cases.

IV. CONCLUSIONS

In this paper, we investigated a method for measuring the Local Barrier Height (LBH) that dates back to the early years of STM research and showed that the quantity measured by this method is undesirably dependent on the feedback controller parameters. We showed that this dependency is due to the fact that the controller still responds, though weakly, to the modulating frequency Ω even if Ω is beyond the bandwidth of the closed-loop system.

On the other hand, we showed that the DC gain of the open-loop plant is solely a function of the LBH. Thus, we proposed a method in Sec. II C to estimate the DC gain and consequently the LBH. We showed that the proposed method removes the dependency of the measured quantity on the feedback parameters as given by Eq. (6).

Since the control loop gain can change due to the LBH variations, we expect that the control system performance is affected by those variations for a fixed set of controller parameters. In order to remove the negative impact of a varying LBH on the system stability and performance, we proposed a tuning algorithm in Sec. II D which continuously updates the PI gains based on the instantaneous LBH measurement.

We conducted an experimental analysis to compare the conventional and proposed LBH measurement methods in Sec. III B. Results show that the proposed method yields LBH images that display the real LBH objects (e.g., dangling bonds) with a better contrast. In other words, the LBH features are better distinguished from the background with our proposed method. Furthermore, we showed that using the PI self-tuning algorithm negatively affects the LBH image obtained by the conventional method. This result is expected given that the conventional LBH measurement method is undesirably dependent on the controller parameters.

We conducted further experiments to investigate the effect of the self-tuning PI controller. We used a set of large but stable PI gains to put the system close to the stability margin. In such a situation, the closed loop is more sensitive to loop gain variations and can present instances of violated stability when the plant DC gain changes due to the LBH. This is exactly what happens over the patterned area in Fig. 3. It is obvious that we can avoid instability by setting low PI gains. However, first, we do this to prove our hypothesis claiming a link between feedback stability and a local property of the tunneling junction that is subject to change. Second, given the large gain variation due to the LBH, it is always possible that instability occurs temporarily even with low PI gains especially while the STM tip triggers chemical reactions on the surface as in the lithography mode. Third, there is always interest toward large PI gains to increase the bandwidth of the closed-loop, and consequently, the scanning speed. Using smaller PI gains reduces the chance of feedback instability, but due to less sensitivity and smaller bandwidth, it results in more tip-sample crash. The proposed PI tuning scheme is expected to facilitate boosting PI gains to the stability limit and hence achieving higher bandwidth and scanning speed while safely avoiding more tip sample crashes.

ACKNOWLEDGMENTS

The authors wish to gratefully acknowledge the financial support of the Air Force Research Laboratory (AFRL) and the Defense Advanced Research Project Agency (DARPA) under AFRL Contract No. FA8650-15-C-7542.

The authors are grateful to Ehud Fuchs and Joshua Ballard of Zyvex Labs for fruitful discussions, and Zyvex Labs' technicians Cyndi Delgado and Robin Santini for their help during the experiments.

[1] G. Binnig and H. Rohrer, "Scanning tunneling microscopy," IBM J. Res. Dev. **44**, 279–293 (2000).
[2] R. A. Wolkow, "Direct observation of an increase in buckled dimers on Si(001) at low temperature," Phys. Rev. Lett. **68**, 2636–2639 (1992).
[3] P. K. Hansma, V. B. Elings, O. Marti, and C. E. Bracker, "Scanning tunneling microscopy and atomic force microscopy: Application to biology and technology," Science **242**, 209–216 (1988).
[4] T. Zhang, P. Cheng, X. Chen, J. F. Jia, X. Ma, K. He, L. Wang, H. Zhang, X. Dai, Z. Fang, X. Xie, and Q. K. Xue, "Experimental demonstration of topological surface states protected by time-reversal symmetry," Phys. Rev. Lett. **103**, 266803 (2009); e-print arXiv:0908.4136.
[5] S. Loth, M. Etzkorn, C. P. Lutz, D. M. Eigler, and A. J. Heinrich, "Measurement of fast electron spin relaxation times with atomic resolution," Science **329**, 1628–1630 (2010).
[6] J. B. Ballard, T. W. Sisson, J. H. G. Owen, W. R. Owen, E. Fuchs, J. Alexander, J. N. Randall, and J. R. Von Ehr, "Multimode hydrogen depassivation lithography: A method for optimizing atomically precise write times," J. Vac. Sci. Technol., B: Microelectron. Nanometer Struct. **31**, 06FC01 (2013).
[7] W. C. T. Lee, S. R. McKibbin, D. L. Thompson, K. Xue, G. Scappucci, N. Bishop, G. K. Celler, M. S. Carroll, and M. Y. Simmons, "Lithography and doping in strained Si towards atomically precise device fabrication," Nanotechnology **25**, 145302 (2014).
[8] A. I. Oliva, E. Anguiano, N. Denisenko, M. Aguilar, and J. L. Penna, "Analysis of scanning tunneling microscopy feedback system," Rev. Sci. Instrum. **66**, 3196 (1995).
[9] N. Lang, "Apparent barrier height in scanning tunneling microscopy," Phys. Rev. B **37**, 10395–10398 (1988).
[10] N. Bonnail, D. Tonneau, F. Jandard, G.-A. Capolino, and H. Dallaporta, "Variable structure control of a piezoelectric actuator for a scanning tunneling microscope," IEEE Trans. Ind. Electron. **51**, 354–363 (2004).
[11] A. I. Oliva, M. Aguilar, J. L. Peña, and E. Anguiano, "Experimental determination of the parameters of the feedback system of a scanning tunnelling microscope," Meas. Sci. Technol. **8**, 501–507 (1997).
[12] B. Voigtlander, *Scanning Probe Microscopy: Atomic Force Microscopy and Scanning Tunneling Microscopy* (Springer-Verlag, Berlin, 2015).
[13] J. W. Lyding, S. Skala, J. S. Hubacek, R. Brockenbrough, and G. Gammie, "Variable-temperature scanning tunneling microscope," Rev. Sci. Instrum. **59**, 1897–1902 (1988).
[14] J. W. Lyding, T. C. Shen, J. S. Hubacek, J. R. Tucker, and G. C. Abeln, "Nanoscale patterning and oxidation of H-passivated Si(100)-2 × 1 surfaces with an ultrahigh vacuum scanning tunneling microscope," Appl. Phys. Lett. **64**, 2010–2012 (1994).
[15] M. Fuechsle, J. A. Miwa, S. Mahapatra, H. Ryu, S. Lee, O. Warschkow, L. C. L. Hollenberg, G. Klimeck, and M. Y. Simmons, "A single-atom transistor," Nat. Nanotechnol. **7**, 242–246 (2012).
[16] B. Weber, S. Mahapatra, H. Ryu, S. Lee, A. Fuhrer, D. L. Thompson, W. C. T. Lee, G. Klimeck, L. C. L. Hollenberg, and M. Y. Simmons, "Ohm's law survives to the atomic scale," Science **335**, 64–67 (2012).
[17] F. Tajaddodianfar, A. Fowler, E. Fuchs, J. N. Randall, and S. O. R. Moheimani, "Frequency-domain closed-loop system identification of a scanning tunneling microscope," in *ASPE 2016 Spring Topical Meeting Precision Mechatronic System Design and Control* (Massachusetts Institute of Technology, Cambridge, Massachusetts, USA, 2016), pp. 54–57.
[18] F. Tajaddodianfar, S. O. R. Moheimani, E. Fuchs, and J. N. Randall, "Stability analysis of a scanning tunneling microscope control system," in *American Control Conference (ACC)* (IEEE, Seattle, WA, USA, 2017), pp. 204–209.

[19]G. Binnig, N. Garcia, H. Rohrer, J. M. Soler, and F. Flores, "Electron-metal-surface interaction potential with vacuum tunneling: Observation of the image force," Phys. Rev. B **30**, 4816–4818 (1984).
[20]Y. Maeda, M. Okumura, S. Tsubota, M. Kohyama, and M. Haruta, "Local barrier height of Au nanoparticles on a TiO_2(1 1 0)-(1 × 2) surface," Appl. Surf. Sci. **222**, 409–414 (2004).
[21]S. S. Aphale, S. Devasia, and S. O. Reza Moheimani, "High-bandwidth control of a piezoelectric nanopositioning stage in the presence of plant uncertainties," Nanotechnology **19**, 125503 (2008).
[22]E. Anguiano, A. I. Oliva, and M. Aguilar, "Optimal conditions for imaging in scanning tunneling microscopy: Theory," Rev. Sci. Instrum. **69**, 3867 (1998).
[23]S. Blanvillain, A. Voda, G. Besançon, and G. Buche, "Subnanometer positioning and drift compensation with tunneling current," IEEE Trans. Control Syst. Technol. **22**, 180–189 (2014).
[24]F. Tajaddodianfar, S. O. R. Moheimani, J. Owen, and J. N. Randall, "A self-tuning controller for high-performance scanning tunneling microscopy," in *IEEE Conference on Control Technology and Applications (CCTA)* (IEEE, Hawaii, USA, 2017), pp. 106–110.
[25]P. A. Ioannou and J. Sun, "*Robust Adaptive Control*" (Prentice Hall, Inc., 1996), p. 821.
[26]M. G. Ruppert, D. M. Harcombe, M. R. Ragazzon, S. O. Reza Moheimani, and A. J. Fleming, "A review of demodulation techniques for amplitude-modulation atomic force microscopy," Beilstein J. Nanotechnol. **8**, 1407–1426 (2017).
[27]Variable Temperature SPM (VT SPM).
[28]J. N. Randall, J. W. Lyding, S. Schmucker, J. R. Von Ehr, J. Ballard, R. Saini, H. Xu, and Y. Ding, "Atomic precision lithography on Si," J. Vac. Sci. Technol., B: Microelectron. Nanometer Struct. **27**, 2764 (2009).
[29]S. Schmucker, N. Kumar, J. Abelson, S. Daly, G. Girolami, M. Bischof, D. Jaeger, R. Reidy, B. Gorman, J. Alexander, J. Ballard, J. Randall, and J. Lyding, "Field-directed sputter sharpening for tailored probe materials and atomic-scale lithography," Nat. Commun. **3**, 935 (2012).
[30]D. Nečas and P. Klapetek, "Gwyddion: An open-source software for SPM data analysis," Cent. Eur. J. Phys. **10**, 181–188 (2012).